

Transition Flow Matching

Chenrui Ma

University of California, Irvine, Irvine, CA 92697, USA
chenrum@uci.edu

Abstract. Mainstream flow matching methods typically focus on learning the local velocity field, which inherently requires multiple integration steps during generation. In contrast, Mean Velocity Flow models establish a relationship between the local velocity field and the global mean velocity, enabling the latter to be learned through a mathematically grounded formulation and allowing generation to be transferred to arbitrary future time points. In this work, we propose a new paradigm that directly learns the transition flow. As a global quantity, the transition flow naturally supports generation in a single step or at arbitrary time points. Furthermore, we demonstrate the connection between our approach and Mean Velocity Flow, establishing a unified theoretical perspective. Extensive experiments validate the effectiveness of our method and support our theoretical claims.

Keywords: Generative Modeling · Flow Matching · Fewer/One-step Generation

1 Introduction

The goal of generative modeling is to transform a prior distribution into the data distribution. Flow Matching [18, 35, 37] provides an intuitive and conceptually simple framework for constructing flow paths that transport one distribution to another. Closely related to diffusion models [1, 4, 45], Flow Matching focuses on learning the velocity fields that guide the generative process during training.

Both Flow Matching [26] and diffusion [45] models rely on iterative sampling during generation. Recently, significant attention has been devoted to few-step—and particularly one-step, feedforward—generative models. One common approach to accelerate Flow/Diffusion models is distillation. However, an ideal solution would allow models to be trained from scratch in an end-to-end manner without relying on pre-trained teachers. Pioneering this direction, Consistency Models [9, 13, 44] introduce a consistency constraint on network outputs for inputs sampled along the same trajectory. Despite their promising performance, this constraint is imposed as a behavioral property of the network, while the properties of the underlying ground-truth field that should guide learning remain unclear [19, 30]. As a result, training can be unstable and typically requires a carefully designed discretization curriculum to progressively constrain the time domain [33, 43, 44]. In contrast, Mean Velocity Models [10, 11, 17, 31, 50] optimize

an objective derived from the relationship between the instantaneous velocity at each time point and the mean velocity toward a future time. This formulation provides a more fundamental and elegant perspective for learning generative dynamics.

In this work, we propose a principled and effective framework, termed **Transition Flow Matching**, for few-step generation with arbitrary numbers of steps and step sizes. Instead of regressing a local vector field as in Flow/Diffusion models [36,37,45], our method directly models the generation trajectory itself, where the transition dynamics naturally represent a global counterpart of velocity. To this end, we derive (with proof) the **Transition Flow Identity**, and propose a principled training objective that enables generative models to satisfy this identity from scratch in an end-to-end manner. This formulation extends and generalizes previous Transition Models [32, 38, 49] and Flow Map methods [3, 40]. Importantly, we further establish a unified perspective that clarifies the relationship between our framework and Mean Velocity methods [10,11]. In experiments, we conduct extensive evaluations, including generation trajectory visualization and image generation tasks across multiple datasets. The results show that our approach achieves competitive performance, demonstrating the effectiveness of modeling transition flows. In addition, we perform ablation studies to analyze key implementation design choices.

Our contributions can be summarized as follows: • We propose Transition Flow Matching, a principled framework for few-step generative modeling. • We derive the Transition Flow Identity and provide a theoretically grounded training objective. • We establish a unified view connecting our method with Mean Velocity models. • We demonstrate competitive performance across multiple image generation benchmarks.

2 Related Works

Flow Matching and Diffusion. Flow Matching [2, 7, 26] and Diffusion [1, 4, 45] models generate samples by parameterizing continuous-time dynamics via Ordinary Differential Equations (ODEs) or Stochastic Differential Equations (SDEs). Flow Matching learns a deterministic velocity field defining an ODE over sample evolution [28], while Diffusion models are typically formulated as SDEs that learn the score function [24]. Through the probability flow ODE formulation, the learned score implicitly defines an equivalent velocity field [27]. In both cases, the learned velocity or score is a local quantity depending only on the current state and time. As a result, generation requires numerical integration over multiple steps to gradually transport samples from noise to data. A common strategy to alleviate trajectory conflicts is distillation [7, 12, 25, 29, 41, 48, 52] from a well-trained Flow or Diffusion model, which provides a better coupling distribution than the standard independent coupling setting [21, 34, 42, 46]. In contrast, our Transition Flow Matching framework directly models global state transitions. Instead of regressing a local vector field, we parameterize mappings between

states at different times, enabling direct transitions from a given state to an arbitrary future state without relying on local velocity regression.

Consistency Model and Mean Velocity Model. To reduce the number of inference steps, Consistency Models [9, 13, 19, 30, 43, 44] learn generation trajectories that maintain consistency over time, enforcing trajectory coherence. Meanwhile, Mean Velocity methods [10, 11, 17, 31, 50] establish a relationship between the instantaneous velocity at each time point and a mean velocity target toward a future time. By contrast, our method directly models the generation trajectory itself, where the transfer dynamics naturally represent a global counterpart of velocity. This enables generation with arbitrary step sizes and arbitrary numbers of steps. Importantly, we establish a unified perspective that clarifies the relationship between our framework and Mean Velocity methods [10, 11].

Transition Models and Flow Map. Transition-based approaches aim to learn state transitions by preserving transition identities. Consistency Trajectory Models [20] learn mappings between arbitrary time steps, but rely on explicit ODE/SDE integration during training. Flow Map Matching [3] regresses zeroth- and first-order derivatives of flow fields, while IMM [53] performs moment matching across time steps. However, these methods either lack sufficient theoretical analysis, do not clearly connect to prior formulations, or rely on distillation. In contrast, our method is trained from scratch in an end-to-end manner and provides a clear theoretical relationship under both the Flow Matching [26] and Mean Velocity frameworks [10, 11].

3 Preliminaries

3.1 Notation and setup

Random variables and realizations. We work in \mathbb{R}^d . Uppercase letters (e.g., X_t, Z) denote random variables (RVs), and lowercase letters (e.g., x_t, z) denote their realizations. For the density of an RV X_t , we write $p_t(\cdot)$, and for a conditional density we write $p_{t|Z}(\cdot | z)$. Expectations are denoted by $\mathbb{E}[\cdot]$.

Source/target distributions and coupling. Let $X_0 \sim p_0$ be the *source* distribution (e.g., standard Gaussian noise) and $X_1 \sim p_1$ be the *target* distribution (e.g., images). A generative model constructs a continuous path of distributions $\{p_t\}_{t \in [0,1]}$ that transports p_0 to p_1 . Let (X_0, X_1) be any coupling with joint density π whose marginals are p_0 and p_1 . Throughout this work, we follow the standard Flow Matching setting where the source and target are independent: $\pi(x_0, x_1) = p_0(x_0)p_1(x_1)$.

Conditioning variable and conditional paths. We use a conditioning RV Z to index conditional paths. Conditioned on $Z = z$, we obtain a conditional path

$\{X_t^Z\}_{t \in [0,1]}$ with conditional density $p_{t|Z}(\cdot | z)$. The corresponding marginal path $\{X_t\}_{t \in [0,1]}$ has density $p_t(\cdot)$ satisfying

$$p_t(x_t) = \int p_{t|Z}(x_t | z) p_Z(z) dz, \quad X_t \sim p_t, \quad X_t | (Z = z) \sim p_{t|Z}(\cdot | z) \quad (1)$$

General interpolant. We consider a general interpolant between the *marginal* endpoints X_0 and X_1 specified by scalar functions $\alpha : [0, 1] \rightarrow \mathbb{R}$ and $\beta : [0, 1] \rightarrow \mathbb{R}$:

$$X_t = \alpha(t) X_0 + \beta(t) X_1, \quad t \in [0, 1]. \quad (2)$$

We assume boundary conditions $\alpha(0) = 1$, $\beta(0) = 0$ and $\alpha(1) = 0$, $\beta(1) = 1$, so that $X_{t=0} = X_0$ and $X_{t=1} = X_1$. If α, β are differentiable, then

$$\frac{d}{dt} X_t = \dot{\alpha}(t) X_0 + \dot{\beta}(t) X_1. \quad (3)$$

Conditioned on $Z = z$, the same schedules induce the conditional path $X_t^Z = \alpha(t) X_0^Z + \beta(t) X_1^Z$ and $\frac{d}{dt} X_t^Z = \dot{\alpha}(t) X_0^Z + \dot{\beta}(t) X_1^Z$.

3.2 Flow Matching

Velocity fields. Let $v(x_t, t | z) \in \mathbb{R}^d$ denote a *conditional* velocity field that transports $p_{t|Z}(\cdot | z)$ over time. The corresponding *marginal* velocity is defined by conditional expectation:

$$v(x_t, t) = \int v(x_t, t | z) p_{Z|t}(z | x_t) dz = \mathbb{E}[v(X_t, t | Z) | X_t = x_t] \quad (4)$$

Generation ODE and continuity equation. A marginal trajectory follows the ODE

$$\frac{dx_t}{dt} = v(x_t, t), \quad t \in [0, 1], \quad (5)$$

and similarly a conditional trajectory follows $\frac{dx_t^z}{dt} = v(x_t, t | z)$. The induced marginal density p_t satisfies the continuity (transport) equation

$$\partial_t p_t(x_t) + \nabla \cdot (p_t(x_t) v(x_t, t)) = 0, \quad t \in [0, 1] \quad (6)$$

and conditioned on $Z = z$, $p_{t|Z}(\cdot | z)$ satisfies

$$\partial_t p_{t|Z}(x_t | z) + \nabla \cdot (p_{t|Z}(x_t | z) v(x_t, t | z)) = 0, \quad t \in [0, 1] \quad (7)$$

Learning Flow Matching. Flow Matching introduces a parameterized model $v^\theta(X_t, t)$ to learn $v(X_t, t)$ by minimizing the marginal loss

$$\mathcal{L}_{\text{MFM}}(\theta) = \mathbb{E}_{t, X_t \sim p_t} D(v(X_t, t), v^\theta(X_t, t)), \quad (8)$$

where $D(\cdot, \cdot)$ is typically a Bregman divergence (e.g., MSE). Since the marginal velocity $v(X_t, t)$ in Eq. (4) is generally intractable, one instead minimizes the conditional loss

$$\mathcal{L}_{\text{CFM}}(\theta) = \mathbb{E}_{t, Z, X_t \sim p_{t|Z}(\cdot | Z)} D(v(X_t, t | Z), v^\theta(X_t, t)) \quad (9)$$

Theorem 1 (Gradient equivalence of Flow Matching [27]). *The gradients of the marginal Flow Matching loss and the conditional Flow Matching loss coincide:*

$$\nabla_{\theta} \mathcal{L}_{\text{MFM}}(\theta) = \nabla_{\theta} \mathcal{L}_{\text{CFM}}(\theta). \quad (10)$$

In particular, the minimizer of the conditional Flow Matching loss is the marginal velocity $v(x_t, t)$.

Remark 1 (Standard Flow Matching). Flow Matching sets the conditioning variable to be the endpoint pair $Z = (X_0, X_1)$. Choosing linear schedules $\alpha(t) = 1 - t$ and $\beta(t) = t$ yields the conditional path $X_t^Z = (1 - t)X_0 + tX_1$ with constant conditional velocity $v(X_t, t | Z) = X_1 - X_0$. Thus Eq. (9) reduces to

$$\mathcal{L}_{\text{FM}}(\theta) = \mathbb{E}_{t, X_0 \sim p_0, X_1 \sim p_1} D\left(X_1 - X_0, v^{\theta}(X_t, t)\right), X_t = (1 - t)X_0 + tX_1 \quad (11)$$

4 Method

Flow Matching learns a time-dependent velocity field $v(x_t, t)$ and generating by integrating the ODE in Eq. (5). Our goal is to directly learn a *transition flow*:

$$X^{\theta}(x_t, t, r) : \mathbb{R}^d \times [0, 1] \times [0, 1] \rightarrow \mathbb{R}^d, \quad 0 \leq t \leq r \leq 1,$$

that maps a state x_t at time t to the *future* state at time r along the same transport dynamics. At inference time, this enables stepping across an arbitrary time grid by repeatedly applying $X^{\theta}(\cdot)$, without explicitly integrating $v(\cdot)$.

4.1 Transition Flow Identity

Average velocity between two time steps. Given the marginal velocity $v(x_{\tau}, \tau)$ as shown in Eq.(4), define the average velocity $u(x_t, t, r)$ for any $0 \leq t \leq r \leq 1$:

$$(r - t)u(x_t, t, r) = x_{t \rightarrow r} - x_t = \int_t^r v(x_{\tau}, \tau) d\tau. \quad (12)$$

Here x_t is the current state at time t , and $x_{t \rightarrow r}$ denotes the marginal transition state at time r obtained by evolving from x_t .

Marginal/conditional transition states. Analogous to Eq. (4), the marginal transition state can be expressed as a conditional expectation:

$$x_{t \rightarrow r} = \int x_{t \rightarrow r}^z p_{Z|t}(z | x_t) dz = \mathbb{E}[X_{t \rightarrow r}^Z | X_t = x_t], \quad (13)$$

where the conditional transition state is $x_{t \rightarrow r}^z = x_t + \int_t^r v(x_{\tau}, \tau | z) d\tau$.

Transition flow. We define the (marginal) transition flow $X(x_t, t, r)$ as the mapping that returns the marginal transition state:

$$X(x_t, t, r) = \int X(x_t, t, r | z) p_{Z|t}(z | x_t) dz = \mathbb{E}[X(X_t, t, r | Z) | X_t = x_t] \quad (14)$$

where $X(x_t, t, r | z) = x_{t \rightarrow r}^z$. Combining Eq. (12) with the definition of $X(\cdot)$ yields

$$u(x_t, t, r) = \frac{x_{t \rightarrow r} - x_t}{r - t} = \frac{X(x_t, t, r) - x_t}{r - t}. \quad (15)$$

Transition Flow Identity. Differentiating Eq. (12) with respect to t (treating r as independent of t) gives

$$u(x_t, t, r) = v(x_t, t) + (r - t) \frac{d}{dt} u(x_t, t, r). \quad (16)$$

Substituting Eq. (15) into Eq. (16) yields the following key identity:

$$\boxed{X(x_t, t, r) = x_{t \rightarrow r} + (r - t) \frac{d}{dt} X(x_t, t, r)} \quad (17)$$

We defer the detailed algebraic derivation to the Appendix.

4.2 Computing the time derivative of a transition flow

To make Eq. (17) actionable for learning, we expand the total derivative $\frac{d}{dt} X(x_t, t, r)$ as:

$$\begin{aligned} \frac{d}{dt} X(x_t, t, r) &= \partial_{x_t} X \cdot \frac{dx_t}{dt} + \partial_t X \cdot \frac{dt}{dt} + \partial_r X \cdot \frac{dr}{dt} \\ &= \partial_{x_t} X \cdot v(x_t, t) + \partial_t X \end{aligned} \quad (18)$$

where $\frac{dx_t}{dt} = v(x_t, t)$ by Eq. (5) and $\frac{dr}{dt} = 0$. In practice, Eq. (18) is given by the Jacobian-vector product (JVP) between the Jacobian matrix of each function ($[\partial_{x_t} X, \partial_t X, \partial_r X]$) and the corresponding tangent vector ($[v, 0, 1]$). For code implementation, modern libraries such as PyTorch provide efficient JVP calculation interfaces.

4.3 Transition Flow Matching objectives

Model parameterization. We introduce a Transition Flow model $X^\theta(x_t, t, r)$ to model $X(x_t, t, r)$. We use $\text{sg}[\cdot]$ to denote a stop-gradient operator (i.e., the argument is treated as a constant target during optimization), and $D(\cdot, \cdot)$ is a Bregman divergence (e.g., MSE).

Intractable marginal objective. Ideally, we would enforce Eq. (17) by minimizing the marginal Transition Flow Matching objective (M-TFM):

$$\mathcal{L}_{\text{M-TFM}}(\theta) = \mathbb{E}_{t, r, X_t \sim p_t} D\left(\text{sg}[X_{\text{tgt}}^{\text{m}}(X_t, t, r)], X^\theta(X_t, t, r)\right), \quad (19)$$

with target

$$X_{\text{tgt}}^{\text{m}}(X_t, t, r) = X_{t \rightarrow r} + (r - t) \frac{d}{dt} X^\theta(X_t, t, r). \quad (20)$$

However, the marginal transition state $X_{t \rightarrow r}$ and the marginal velocity $v(x_t, t)$ (needed inside $\frac{d}{dt} X^\theta$ via Eq. (18)) are generally intractable, hence Eq. (19) cannot be evaluated directly.

Tractable conditional objective. Instead, we minimize a conditional Transition Flow Matching objective (C-TFM):

$$\mathcal{L}_{\text{C-TFM}}(\theta) = \mathbb{E}_{t, r, Z, X_t \sim p_{t|Z}(\cdot|Z)} D\left(\text{sg}[X_{\text{tgt}}^{\text{c}}(X_t, t, r | Z)], X^\theta(X_t, t, r)\right), \quad (21)$$

where the conditional target is

$$X_{\text{tgt}}^{\text{c}}(X_t, t, r | Z) = X_{t \rightarrow r}^Z + (r - t) \frac{d}{dt} X^\theta(X_t, t, r). \quad (22)$$

Crucially, under appropriate choices of Z and the conditional path construction, both the conditional transition state $X_{t \rightarrow r}^Z$ and the conditional velocity $v(x_t, t | Z)$ become tractable, which makes $\frac{d}{dt} X^\theta$ computable via Eq. (18).

Theorem 2 (Gradient equivalence of Transition Flow Matching). *See the proof in the Appendix. The gradients of the marginal and conditional Transition Flow Matching losses coincide:*

$$\nabla_\theta \mathcal{L}_{\text{M-TFM}}(\theta) = \nabla_\theta \mathcal{L}_{\text{C-TFM}}(\theta). \quad (23)$$

In particular, the minimizer of the conditional objective regresses $X^\theta(X_t, t, r)$ toward the marginal target $X_{\text{tgt}}^{\text{m}}(X_t, t, r)$, which is defined to satisfy the Transition Flow Identity in Eq. (17).

4.4 Training and inference procedure

Remark 2 (Standard Transition Flow Matching). We adopt the standard Flow Matching setting in Remark 1 by taking $Z = (X_0, X_1)$ and using the linear interpolant

$$X_t = (1 - t)X_0 + tX_1, \quad 0 \leq t \leq 1.$$

For any $0 \leq t \leq r \leq 1$, the conditional transition state is

$$X_{t \rightarrow r}^Z = (1 - r)X_0 + rX_1,$$

Algorithm 1 Transition Flow Matching (TFM): Training

```

// jvp returns (output, JVP)
// tfm predicts  $X^\theta(x_t, t, r)$ 
x_1 = sample_batch(), x_0 = randn_like(x_1), (t,r)=sample_t_r()
//  $0 \leq t \leq r \leq 1$ 
x_t = (1-t)x_0 + t x_1, v = x_1 - x_0
x_t_to_r = (1-r)x_0 + r x_1
(X, dX_dt) = jvp(tfm, (x_t,t,r),(v,1,0))
X_tgt = x_t_to_r + (r-t)dX_dt
loss = metric(X - stopgrad(X_tgt))
return loss

```

and the conditional velocity is constant:

$$v(X_t, t | Z) = X_1 - X_0.$$

Under this instantiation, the tractable Transition Flow Matching objective in Eq. (21) becomes

$$\mathcal{L}_{\text{TFM}}(\theta) = \mathbb{E}_{t, r, Z, X_t \sim p_{t|Z}(\cdot|Z)} D\left(\text{sg}[X_{t \rightarrow r}^Z + (r-t)\frac{d}{dt}X^\theta(X_t, t, r)], X^\theta(X_t, t, r)\right), \quad (24)$$

The time derivative term $\frac{d}{dt}X^\theta(X_t, t, r)$ extends Eq. (18) by incorporating the tractable conditional velocity, and is given by (see the proof in Appendix):

$$\frac{d}{dt}X^\theta(X_t, t, r) = \partial_{x_t}X^\theta(X_t, t, r) \cdot v(X_t, t | Z) + \partial_t X^\theta(X_t, t, r). \quad (25)$$

During inference, we recursively apply the model to transform the generation trajectory from the source distribution to the target distribution:

$$\hat{x}_r = X^\theta(x_t, t, r) \quad (26)$$

For clarity, we summarize the conceptual training procedures in the Algorithm.1.

4.5 Classifier-Free Guidance

Transition Flow Matching naturally supports classifier-free guidance (CFG) via

$$X_{\text{cfg}}^\theta(x_t, t, r | \mathbf{c}) = \omega X(x_t, t, r | \mathbf{c}) + (1 - \omega)X(x_t, t, r | \emptyset). \quad (27)$$

This forms a combination of the class-conditional transition flow $X(x_t, t, r | \mathbf{c})$ and the unconditional transition flow $X(x_t, t, r | \emptyset)$, allowing us to control the strength of class conditioning at inference time by tuning ω . Here, the term “condition” refers specifically to class conditioning, which is distinct from the marginal/conditional distinction used in previous sections. Following standard

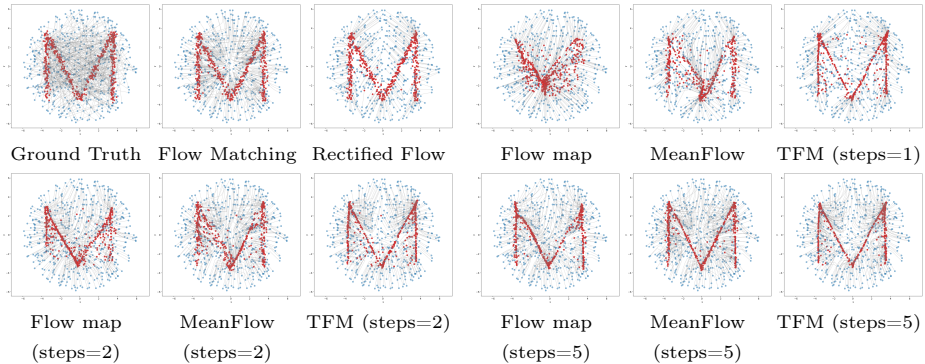


Fig. 1: *2D Generation Trajectory Visualization on Synthetic Data.* Tested methods include: Flow Matching [26], Rectified Flow [29], Flow Map Matching [3], MeanFlow [10].

CFG practice [16], we train a single model $X^\theta(\cdot)$ that supports both class-conditional generation $X^\theta(\cdot | \mathbf{c})$ and unconditional generation $X^\theta(\cdot | \emptyset)$. Concretely, for conditional training, the endpoint X_1 in Sec. 4.4 is sampled from the class-conditional target distribution $p_1(\cdot | \mathbf{c})$; for unconditional training, X_1 in Sec. 4.4 is sampled from the unconditional target distribution $p_1(\cdot)$.

5 Implementation Design

Loss Metrics. In Eq. (24), the Bregman divergence $D(\cdot, \cdot)$ is instantiated as the squared ℓ_2 loss. Following [10], we further investigate alternative loss metrics. In general, we consider loss functions of the form $\mathcal{L} = \|\Delta\|_2^{2\gamma}$, where Δ denotes the regression error. It can be shown (see [13]) that minimizing $\|\Delta\|_2^{2\gamma}$ is equivalent to minimizing the squared ℓ_2 loss $\|\Delta\|_2^2$ with *adapted loss weights*. In practice, we define the weight as $w = \frac{1}{(\|\Delta\|_2^2 + c)^p}$, where $p = 1 - \gamma$ and $c > 0$ is a small constant (e.g., 10^{-3}) for numerical stability. The resulting adaptively weighted loss takes the form $\text{sg}(w) \cdot \mathcal{L}$, with $\mathcal{L} = \|\Delta\|_2^2$. When $p = 0.5$, this formulation resembles the Pseudo-Huber loss [43]. We compare different choices of p in the experiments.

Sampling Time Steps (t, r) . We sample the two time steps (t, r) from a predefined logit-normal (lognorm) distribution [8, 10]. Specifically, we first draw a sample from a normal distribution $\mathcal{N}(\mu, \sigma)$ and map it to the interval $(0, 1)$ via the logistic function to obtain t . We then sample another logit-normal variable d in the same manner and set $r = t + d(1 - t)$, which ensures that the constraint $0 \leq t \leq r \leq 1$ is satisfied. Note that for any given t , the transition time r is obtained by an affine transformation of a logit-normal random variable, ensuring that $r \in [t, 1]$ while preserving a logit-normal-shaped density over the valid interval. Different hyperparameter settings of the logit-normal distribution are evaluated in the experiments.

Conditioning on (t, r) . We employ positional embeddings [10, 47] to encode the time variables, which are subsequently combined and used as conditioning inputs to the neural network. Although the vector field is parameterized as $X_\theta(x_t, t, r)$, it is not strictly necessary for the network to directly condition on (t, r) . For instance, the network can instead condition on $(t, \Delta t)$, where $\Delta t = r - t$. In this case, we define $X_\theta(\cdot, t, r) \triangleq \text{net}(\cdot, t, r - t)$, with net denoting the neural network. The Jacobian-vector product (JVP) is always computed with respect to the function $X_\theta(\cdot, t, r)$. We empirically compare different conditioning strategies in the experiments.

6 Experiments

6.1 Synthetic Data and Visualization

Synthetic data experiments are conducted to visualize the results and intuitively demonstrate the effectiveness of the proposed method [36, 51]. We simulate and visualize the generation trajectories of different methods on a 2D alphabet ‘‘M’’ dataset, as shown in Figure 1. In this dataset, the source distribution (blue points) is circular, while the target distribution (red points) forms the shape of the letter ‘‘M’’. The visualization results are consistent with the discussion in the previous section: our goal is to enable generation with arbitrary step sizes and an arbitrary number of steps by modeling the generation trajectory. Notably, even one-step generation shows promising results.

6.2 Visual Generation

CIFAR-10. CIFAR-10 is a 32×32 resolution image dataset containing multiple classes and is a widely used benchmark in generative modeling [22]. For a fair evaluation, we adopt the same UNet architecture and training protocol as in prior work [13, 14], while replacing the conventional flow matching objective with the proposed *Transition Flow Matching* objective as defined in Eq. (24).

The UNet model X^θ follows a standard encoder–decoder design with residual blocks and skip connections. A self-attention block is inserted after the residual block at 16×16 resolution and at the bottleneck layer. The model takes the current state x_t and the time variables (t, r) as input, where (t, r) are embedded and used to modulate adaptive group normalization layers through learnable scale and shift parameters.

To quantitatively evaluate the generation performance, we compare our method with several state-of-the-art approaches by measuring the generation quality using the Fréchet Inception Distance (FID) [15], computed under varying NFE: [1, 2, 5, 10] and adaptive-step Dopri5 ODE solver [5], as presented in Table 1. The results in Table 1 show that our method achieves the best performance in one-step generation (NFE = 1). Moreover, the FID score consistently decreases as NFE increases, while both Consistency Models and Mean Velocity Models tend to exhibit degraded performance with higher NFE values.

	NFE / Sampler	# Params.	1	2	5	10
Flow	Flow Matching [26] [ICLR'23]	36.5M	-	166.65	36.19	14.4
	VFM [14] [ICML'25]	60.6M	-	97.83	13.12	5.34
Re-Flow	1-Rectified Flow [29] [ICLR'23]	36.5M	378	6.18	-	-
	2-Rectified Flow [29] [ICLR'23]	36.5M	12.21	4.85	-	-
	3-Rectified Flow [29] [ICLR'23]	36.5M	8.15	5.21	-	-
Mean Velocity / Consistency	CT [44] [ICML'23]	61.8M	8.71	5.32	11.412	23.948
	iCT [43] [ICLR'24]	55M	2.83	2.46	-	-
	ECT [13] [ICLR'25]	55M	3.60	2.11	-	-
	sCT [30] [ICLR'25]	55M	2.85	2.06	-	-
	IMM [53] [ICML'25]	55M	3.20	1.98	-	-
	MeanFlow [10] [NeurIPS'25]	55M	2.92	2.23	2.84	2.27
	S-VFM [36] [CVPR'26]	60.6M	2.81	2.16	2.02	1.97
	TFM [Ours]	55M	2.77	2.08	1.96	1.91

Table 1: Quantitative Comparison with Different Generation Methods on CIFAR-10 Dataset. Our method achieves the best performance in one-step generation (NFE = 1). Moreover, the FID score consistently decreases as NFE increases.



Fig. 2: Generation Results on ImageNet-256 under Varying NFE. As the number of function evaluations (NFE) increases from 1 to 10, the generated images exhibit progressively improved detail and fidelity. Notably, even single-step generation already produces reasonably good results.

ImageNet. To evaluate robustness and scalability on large-scale data, we conduct experiments on the ImageNet dataset with image resolution 256×256 [23]. All experiments are performed on class-conditional ImageNet generation at this resolution. Following common practice, we evaluate the Fréchet Inception Distance (FID) [15] on 50K randomly generated images. Following prior works [9, 14, 36], we implement all models in the latent space of a pre-trained VAE tokenizer [39]. For 256×256 images, the tokenizer maps images into a latent representation of size $32 \times 32 \times 4$, which serves as the input to the generative model. All models are trained from scratch under identical data and optimization settings.

As the backbone architecture, we adopt MeanFlow [10], a transformer-based model that has demonstrated strong performance in high-resolution image generation. For fair comparison, we strictly follow the original MeanFlow [10] training recipe and optimization settings, modifying only the learning objective.

Method	# Params.	NFE	FID
iCT-XL/2 [43] [ICLR'24]	675M	1	34.24
Shortcut-XL/2 [9] [ICLR'25]	675M	1	10.60
MeanFlow-XL/2 [10] [NeurIPS'25]	676M	1	3.43
S-VFM-XL/2 [36] [CVPR'26]	677M	1	3.31
TFM-XL/2 [Ours]	676M	1	3.02
iCT-XL/2 [43] [ICLR'24]	675M	2	20.30
iMM-XL/2 [53] [ICML'25]	675M	1×2	7.77
MeanFlow-XL/2 [10] [NeurIPS'25]	676M	2	2.93
S-VFM-XL/2 [36] [CVPR'26]	677M	2	2.86
TFM-XL/2 [Ours]	676M	2	2.77

Table 2: *Quantitative Comparison with Different Generation Methods on ImageNet 256 × 256 Dataset.* Our method achieves the best performance in few-step generation.

Specifically, we introduce **TFM**, which is parameterized by $X^\theta(X_t, t, r)$, by replacing the original velocity-based loss with the proposed Transition Flow Matching loss in Eq. (24). The model is trained to directly predict the transition flow $X(x_t, t, r)$ rather than the local velocity field. Both time variables t and r are embedded and injected into the transformer blocks via adaptive normalization layers.

During training, we sample (X_0, X_1) pairs from the data distribution and construct linear interpolants following the standard Flow Matching setting. Given a randomly sampled time pair (t, r) with $0 \leq t \leq r \leq 1$, the network is trained to regress the transition flow using the tractable Transition Flow Matching objective described in Eq. (24), which enforces consistency with the Transition Flow Identity. At inference time, sample generation is performed by repeatedly applying the learned transition flow across a predefined time grid, starting from Gaussian noise. This formulation allows the model to directly predict future states along the transition trajectory, enabling flexible and efficient generation.

Figure 2 illustrates generation results under different numbers of function evaluations (NFE), using distinct initial noise. Within each row, images at the same spatial location across different panels are generated from the same initial noise realization. Each column corresponds to a different NFE setting, with NFE values of [1, 2, 5, 10] arranged from top to bottom. As the number of function evaluations increases, the generated images exhibit improved visual fidelity and structural coherence. Notably, even one-step generation (NFE = 1) produces competitive samples, supporting the claim that the transition flow model $X^\theta(X_t, t, r)$ learns to predict the future state at r from the current state X_t at time t , thereby enabling effective few-step sampling.

Following standard evaluation protocols, we randomly generate 50K images from each model and report the corresponding FID scores in Table 2. TFM-XL consistently outperforms both Consistency Models and Mean Velocity Models under identical training settings. These results demonstrate that explicitly modeling *global transition dynamics* through a transition flow—capable of predicting arbitrary future states—rather than learning a naturally local velocity field, provides greater flexibility in simulation steps for flow- and diffusion-based generation methods.

We further analyze the training dynamics by comparing TFM with SiT and MeanFlow across different training iterations, as shown in Figure 3e. For SiT,

we follow the default inference setting with $\text{NFE} = 250$, while for both TFM and MeanFlow we use $\text{NFE} = 1$ to reflect their one-step generation capability. The results show that TFM achieves clear performance improvements once sufficiently trained, and the training curves indicate that performance consistently improves as the number of training epochs increases. This behavior confirms the effectiveness and scalability of the proposed transition flow formulation in both training and inference.

6.3 Ablation Study

In our ablation study, we use the ViT-B/4 architecture [6] ("Base" size with a patch size of 4 as developed in [37]), trained for 80 epochs (400K iterations).

Conditioning on (t, r) . Following the model parameterization in Sec. 5, the transition flow $X_\theta(x_t, t, r)$ requires explicit conditioning on the temporal variables. Similar to prior designs, we encode time information through positional embeddings and study different conditioning strategies that share the same functional form but differ in the specific choice of variables. Concretely, instead of directly conditioning on (t, r) , the network can equivalently condition on $(t, \Delta t)$ with $\Delta t = r - t$, leading to the parameterization $X_\theta(\cdot, t, r) \triangleq \text{net}(\cdot, t, r - t)$. We compare these variants in Tab. 3a. The results indicate that all studied conditioning forms lead to stable and effective one-step generation, demonstrating that our transition flow formulation is robust to the exact choice of temporal embedding. Conditioning on $(t, \Delta t)$ yields the strongest performance overall, while directly using (t, r) performs comparably. Notably, even conditioning solely on the interval Δt produces competitive results, suggesting that relative temporal information plays a dominant role in our method.

Sampling Time Steps (t, r) . The choice of the sampling distribution for time steps is known to have a significant impact on generation quality. In our framework, we sample (t, r) using logit-normal distributions, consistent with the implementation described in Sec. 5. Specifically, we consider two logit-normal distributions: one for sampling the base time t and another for sampling the relative offset that determines r . This design ensures $0 \leq t \leq r \leq 1$ by construction while allowing flexible control over the density of sampled time pairs. We evaluate different hyperparameter settings of these logit-normal samplers in Tab. 3d. The results show that logit-normal sampling consistently outperforms alternative choices, aligning with observations reported in prior flow-matching-based methods.

Loss Metrics. As discussed in Sec. 5, our training objective adopts a Bregman divergence instantiated via adaptively weighted squared ℓ_2 loss. While the overall loss formulation remains the same across experiments, we vary the exponent p that controls the adaptive weighting, which effectively changes the loss metric. The corresponding results are summarized in Tab. 3b. We find that $p = 1$ achieves the best overall performance, indicating a strong benefit from aggressive

pos. embed	FID, 1-NFE
(t, r)	60.12
$(t, t - r)$	59.87
$(t, r, t - r)$	62.48
$t - r$ only	62.16

(a) *Positional embedding.* The network is conditioned on the embeddings applied to the specified variables.

p	FID, 1-NFE
0.0	79.76
0.5	62.47
1.0	59.87
1.5	65.68
2.0	69.26

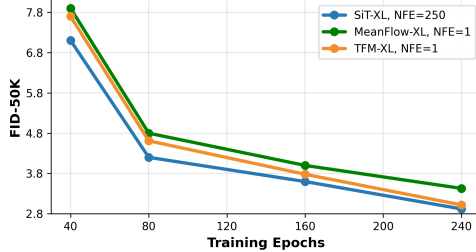
(b) *Loss metrics.* $p = 0$ is squared L2 loss. $p = 0.5$ is Pseudo-Huber loss.

ω	FID, 1-NFE
1.0 (w/o cfg)	61.06
1.5	32.51
2.0	19.05
3.0	14.76
5.0	20.12

(c) *CFG scale.* Our method supports 1-NFE CFG sampling.

t, r sampler	FID, 1-NFE
uniform(0, 1)	65.73
lognorm(-0.2, 1.0)	63.56
lognorm(-0.2, 1.2)	62.27
lognorm(-0.4, 1.0)	59.87
lognorm(-0.4, 1.2)	59.94

(d) *Time samplers.* t and r are sampled from the specific sampler.



(e) *Comparison of FID-50K Score over Training Iterations on ImageNet 256×256 Dataset.*

Table 3: *Ablation study on 1-NFE ImageNet 256×256 generation.* FID-50K is evaluated. Default configurations are: B/4 backbone, 80-epoch training from scratch.

adaptive weighting. Setting $p = 0.5$, which resembles the Pseudo-Huber loss, also yields competitive results. In contrast, the standard squared ℓ_2 loss ($p = 0$) underperforms relative to other choices, though it still leads to meaningful one-step generation. These trends are consistent with prior findings on the importance of loss reweighting for few-step or single-step generative models.

Guidance Scale. We further investigate the effect of classifier-free guidance (CFG) within our transition flow framework. The results, reported in Tab. 3c, show that increasing the guidance scale significantly improves generation quality. This behavior is consistent with observations in multi-step diffusion and flow models. Importantly, our CFG formulation, introduced in Sec. 5, is fully compatible with one-step (1-NFE) sampling and does not introduce additional inference cost beyond a constant factor.

7 Conclusion

In this work, we introduced **Transition Flow Matching**, a principled framework for few-step generative modeling. Instead of learning local velocity fields as in conventional Flow/Diffusion models, our method directly models the generation trajectory through transition dynamics, providing a global perspective on generative flows. We derive the **Transition Flow Identity** and develop a theoretically grounded objective that enables end-to-end training from scratch, while also establishing a unified view that connects our framework with Mean Velocity methods.

8 Proof of Transition Identity

8.1 Notation and Preliminary

Random variables and realizations. We work in \mathbb{R}^d . Uppercase letters (e.g., X_t, Z) denote random variables (RVs), and lowercase letters (e.g., x_t, z) denote their realizations (points/values). For a density (or probability law) of an RV X_t , we write $p_t(\cdot)$, and for a conditional density we write $p_{t|Z}(\cdot | z)$. Expectations are denoted by $\mathbb{E}[\cdot]$.

Source/target distributions and coupling. Let $X_0 \sim p_0$ be the *source* distribution (e.g., standard Gaussian noise) and $X_1 \sim p_1$ be the *target* distribution (e.g., images). A generative model constructs a continuous path of distributions $\{p_t\}_{t \in [0,1]}$ that transports p_0 to p_1 . Let (X_0, X_1) be any coupling on \mathbb{R}^d with joint density π whose marginals are p_0 and p_1 (not necessarily independent). In this work, we follow the standard Flow Matching setting, the *source* and the *target* distributions are independent: $\pi(x_0, x_1) = p_0(x_0)p_1(x_1)$.

Conditioning variable and conditional paths [26]. We use a conditioning RV Z to index conditional paths. Conditioned on $Z = z$, we obtain conditional coupling (X_0^Z, X_1^Z) and a conditional path $\{X_t^Z\}_{t \in [0,1]}$ with conditional density $p_{t|Z}(\cdot | z)$. The marginal path is $\{X_t\}_{t \in [0,1]}$, with density $p_t(\cdot)$, satisfying:

$$p_t(x_t) = \int p_{t|Z}(x_t | z) p_Z(z) dz, \quad X_t \sim p_t, \quad X_t | (Z = z) \sim p_{t|Z}(\cdot | z). \quad (28)$$

Interpolant. We consider a general interpolant between the *marginal* endpoints X_0 and X_1 , specified by scalar functions $\alpha : [0, 1] \rightarrow \mathbb{R}$ and $\beta : [0, 1] \rightarrow \mathbb{R}$:

$$X_t = \alpha(t) X_0 + \beta(t) X_1, \quad t \in [0, 1]. \quad (29)$$

We assume the boundary conditions $\alpha(0) = 1$, $\beta(0) = 0$ and $\alpha(1) = 0$, $\beta(1) = 1$, so that $X_{t=0} = X_0$ and $X_{t=1} = X_1$. If α, β are differentiable, then

$$\frac{d}{dt} X_t = \dot{\alpha}(t) X_0 + \dot{\beta}(t) X_1. \quad (30)$$

Conditioned on $Z = z$, the same schedules induce the conditional path $X_t^Z = \alpha(t) X_0^Z + \beta(t) X_1^Z$ and $\frac{d}{dt} X_t^Z = \dot{\alpha}(t) X_0^Z + \dot{\beta}(t) X_1^Z$.

Flow Matching vector fields [26]. Let $v(x_t, t | z) \in \mathbb{R}^d$ denote a *conditional* velocity field that transports the conditional density $p_{t|Z}(\cdot | z)$ along time. The corresponding *marginal* velocity field is defined by conditional expectation:

$$v(x_t, t) = \int v(x_t, t | z) p_{Z|t}(z | x_t) dz = \mathbb{E}[v(X_t, t | Z) | X_t = x_t]. \quad (31)$$

A marginal trajectory, i.e., Flow Matching generation trajectory, follows the ODE:

$$\frac{dx_t}{dt} = v(x_t, t), \quad t \in [0, 1], \quad (32)$$

and similarly a conditional trajectory follows $\frac{dx_t^z}{dt} = v(x_t, t | z)$.

Continuity (transport) equations [26, 27]. The evolution of densities induced by these velocity fields is characterized by the continuity (transport) equation. For the marginal density p_t ,

$$\partial_t p_t(x_t) + \nabla \cdot (p_t(x_t) v(x_t, t)) = 0, \quad t \in [0, 1]. \quad (33)$$

Conditioned on $Z = z$, the conditional density $p_{t|Z}(\cdot | z)$ satisfies

$$\partial_t p_{t|Z}(x_t | z) + \nabla \cdot (p_{t|Z}(x_t | z) v(x_t, t | z)) = 0, \quad t \in [0, 1]. \quad (34)$$

Flow Matching learns a parameterized velocity field (or equivalent dynamics) so that the induced marginal path $\{p_t\}$ solves Eq. (33) with boundary conditions $p_{t=0} = p_0$ and $p_{t=1} = p_1$.

Learning Flow Matching. Flow Matching introduce a velocity field model $v^\theta(X_t, t)$ to learn $v(X_t, t)$, ideally, by minimizing the marginal Flow Matching loss:

$$\mathcal{L}_{\text{MFM}}(\theta) = \mathbb{E}_{t, X_t \sim p_t} D\left(v(X_t, t), v^\theta(X_t, t)\right) \quad (35)$$

However, since the marginal velocity $v(X_t, t)$ in Eq.(31) is not tractable, so the marginal loss Eq.(35) above cannot be computed as is. Instead, we minimize the conditional Flow Matching loss:

$$\mathcal{L}_{\text{CFM}}(\theta) = \mathbb{E}_{t, Z, X_t \sim p_{t|Z}(\cdot | Z)} D\left(v(X_t, t | Z), v^\theta(X_t, t)\right) \quad (36)$$

The two losses Eq.(35) and Eq.(36) are equivalent for learning purposes, since their gradients coincide:

Theorem 3 (Gradient equivalence of Flow Matching [27]). *The gradients of the marginal Flow Matching loss and the conditional Flow Matching loss coincide:*

$$\nabla_\theta \mathcal{L}_{\text{MFM}}(\theta) = \nabla_\theta \mathcal{L}_{\text{CFM}}(\theta) \quad (37)$$

In particular, the minimizer of the conditional Flow Matching loss is the marginal velocity $v(x_t, t)$.

Remark 3 (Standard Flow Matching). Flow Matching sets the conditioning variable to be the endpoint pair

$$Z = (X_0, X_1),$$

so that conditioning on $Z = z$ fixes the endpoint pair $(X_0^Z, X_1^Z) = (X_0, X_1)$. Choosing the linear schedules $\alpha(t) = 1 - t$ and $\beta(t) = t$ yields the conditional path

$$X_t^Z = (1 - t)X_0^Z + tX_1^Z = (1 - t)X_0 + tX_1, \quad 0 \leq t \leq 1$$

hence the time-derivative of this conditional path is constant:

$$\frac{d}{dt} X_t^Z = X_1^Z - X_0^Z = X_1 - X_0.$$

Therefore, for $Z = (X_0, X_1)$, the conditional velocity used as supervision in the conditional Flow Matching loss is a constant:

$$v(X_t, t | Z) = X_1^Z - X_0^Z = X_1 - X_0,$$

With this setup, the Flow Matching objective in Eq. (36) can be written explicitly as

$$\mathcal{L}_{\text{FM}}(\theta) = \mathbb{E}_{t, X_0 \sim p_0, X_1 \sim p_1} D\left(X_1 - X_0, v^\theta(X_t, t)\right), \quad X_t = (1-t)X_0 + tX_1,$$

i.e., one samples $t \sim \text{Unif}[0, 1]$, draws independent endpoints $X_0 \sim p_0$ and $X_1 \sim p_1$, forms the interpolated state X_t , and regresses the model $v^\theta(X_t, t)$ to the constant target $X_1 - X_0$. By Theorem 3, minimizing this conditional loss yields the marginal velocity field $v(x_t, t)$ in Eq. (31).

8.2 Transition Flow Identity

To connect with previous works [10, 11], we define the average velocity $u(x_t, t, r)$ as:

$$(r-t)u(x_t, t, r) = x_{t \rightarrow r} - x_t = \int_t^r v(x_\tau, \tau) d\tau \quad 0 \leq t \leq r \leq 1 \quad (38)$$

where $v(x_\tau, \tau)$ is the marginal velocity of Flow Matching in time step $\tau \in [0, 1]$ for state x_τ , as shown in Eq.(31).

In Eq.(38), x_t is the current state at time step t , $x_{t \rightarrow r}$ is the transition state at time step r , which comes from x_t at time step t .

$$x_{t \rightarrow r} = x_t + \int_t^r v(x_\tau, \tau) d\tau \quad (39)$$

Note here, akin to the marginal velocity of Flow Matching $v(x_t, t)$ as Eq.(31), $x_{t \rightarrow r}$ is the marginal transition state:

$$x_{t \rightarrow r} = \int x_{t \rightarrow r}^z p_{Z|t}(z | x_t) dz = \mathbb{E}[X_{t \rightarrow r}^Z | X_t = x_t] \quad (40)$$

where $x_{t \rightarrow r}^z$ is the conditional transition state:

$$x_{t \rightarrow r}^z = x_t + \int_t^r v(x_\tau, \tau | z) d\tau \quad (41)$$

The average velocity $u(x_t, t, r)$ is the displacement between two time steps t and r divided by the time interval $r - t$:

$$u(x_t, t, r) \triangleq \frac{1}{r-t} \int_t^r v(x_\tau, \tau) d\tau \quad (42)$$

Differentiate both sides of Eq.(38) with respect to t , treating r as independent of t . We have:

$$\frac{d}{dt}(r-t)u(x_t, t, r) = \frac{d}{dt} \int_t^r v(x_\tau, \tau) d\tau \implies u(x_t, t, r) = v(x_t, t) + (r-t) \frac{d}{dt} u(x_t, t, r) \quad (43)$$

Our learning target is the Transition Flow $X(x_t, t, r)$ that transit state x_t at time step t to $x_{t \rightarrow r}$ at time step r : $X(x_t, t, r) = x_{t \rightarrow r}$, which yield:

$$X(x_t, t, r) = \int X(x_t, t, r | z) p_{Z|t}(z | x_t) dz = \mathbb{E}[X(X_t, t, r | Z) | X_t = x_t] \quad (44)$$

where $X(x_t, t, r | z) = x_{t \rightarrow r}^z$ is conditional transition state. Note that Eq.(44) is identical to Eq.(40).

From Eq.(38), we build the association between the average velocity and the Transition Flow (transition state):

$$u(x_t, t, r) = \frac{x_{t \rightarrow r} - x_t}{r - t} = \frac{X(x_t, t, r) - x_t}{r - t} \quad (45)$$

Substitute Eq.(45) into Eq.(43), we obtain the following equation:

$$\frac{X(x_t, t, r) - x_t}{r - t} = v(x_t, t) + (r - t) \frac{d}{dt} \left(\frac{X(x_t, t, r) - x_t}{r - t} \right) \quad (46)$$

where r is independent of t , and the time derivative of x_t is marginal velocity $v(x_t, t)$, given by Eq.(32).

Define the time derivative of the fraction:

$$A(t) := \frac{X(x_t, t, r) - x_t}{r - t}.$$

Using the quotient rule and the fact that r is constant, we obtain

$$\frac{dA}{dt} = \frac{(r - t) \frac{d}{dt}(X(x_t, t, r) - x_t) + (X(x_t, t, r) - x_t)}{(r - t)^2}.$$

Since

$$\frac{d}{dt}(X(x_t, t, r) - x_t) = \frac{dX(x_t, t, r)}{dt} - v(x_t, t),$$

we have

$$\frac{dA}{dt} = \frac{(r - t) \left(\frac{dX(x_t, t, r)}{dt} - v(x_t, t) \right) + (X(x_t, t, r) - x_t)}{(r - t)^2}.$$

The right-hand side of Eq.(46) becomes

$$\begin{aligned} v(x_t, t) + (r - t) \frac{dA}{dt} &= v(x_t, t) + \frac{(r - t) \left(\frac{dX(x_t, t, r)}{dt} - v(x_t, t) \right) + (X(x_t, t, r) - x_t)}{r - t} \\ &= v(x_t, t) + \frac{dX(x_t, t, r)}{dt} - v(x_t, t) + \frac{X(x_t, t, r) - x_t}{r - t} \\ &= \frac{dX(x_t, t, r)}{dt} + \frac{X(x_t, t, r) - x_t}{r - t} \end{aligned} \quad (47)$$

Comparing both sides of Eq.(46) yields

$$\begin{aligned} \frac{X(x_t, t, r) - x_t}{r - t} &= \frac{dX(x_t, t, r)}{dt} + \frac{X(x_t, t, r) - x_t}{r - t} \\ X(x_t, t, r) &= X(x_t, t, r) + (r - t) \frac{dX(x_t, t, r)}{dt} \end{aligned} \quad (48)$$

Given $X(x_t, t, r) = x_{t \rightarrow r}$, the **Transition Flow Identity** can be shown as:

$$\boxed{X(x_t, t, r) = x_{t \rightarrow r} + (r - t) \frac{d}{dt} X(x_t, t, r)} \quad (49)$$

8.3 Calculate Time Derivative of Transition Flow

To compute the $\frac{d}{dt} X(x_t, t, r)$ term, we expand it in terms of partial derivatives:

$$\begin{aligned} \frac{d}{dt} X(x_t, t, r) &= \partial_{x_t} X \cdot \frac{dx_t}{dt} + \partial_t X \cdot \frac{dt}{dt} + \partial_r X \cdot \frac{dr}{dt} \\ &= \partial_{x_t} X \cdot v(x_t, t) + \partial_t X \cdot 1 + \partial_r X \cdot 0 \\ &= \partial_{x_t} X \cdot v(x_t, t) + \partial_t X \end{aligned} \quad (50)$$

where $\frac{dx_t}{dt} = v(x_t, t)$ as shown in Eq.(32). The time derivative shown in Eq. (50) is given by the Jacobian-vector product (JVP) between the Jacobian matrix of each function ($[\partial_{x_t} X, \partial_t X, \partial_r X]$) and the corresponding tangent vector ($[v, 0, 1]$). For code implementation, modern libraries such as PyTorch provide efficient JVP calculation interfaces.

8.4 Towards Tractable Transition Flow Matching Objective

Up to this point, the formulations are independent of any network parameterization. We now introduce the Transition Flow model $X^\theta(x_t, t, r)$, parameterized by θ , to learn $X(x_t, t, r)$. Formally, we encourage $X^\theta(x_t, t, r)$ to satisfy the **Transition Flow Identity** as Eq.(49). To this end, ideally, we can minimize the marginal Transition Flow Matching objective (M-TFM):

$$\mathcal{L}_{\text{M-TFM}}(\theta) = \mathbb{E}_{t, r, X_t \sim p_t} D\left(\text{sg}[X_{\text{tgt}}^{\text{m}}(X_t, t, r)], X^\theta(X_t, t, r)\right) \quad (51)$$

$$\text{where } X_{\text{tgt}}^{\text{m}}(X_t, t, r) = X_{t \rightarrow r} + (r - t) \frac{d}{dt} X^\theta(X_t, t, r) \quad (52)$$

where $D(\cdot)$ represents a Bregman divergence (e.g MSE) to regress our learnable Transition Flow $X^\theta(x_t, t, r)$ onto the target $X_{\text{tgt}}^{\text{m}}(x_t, t, r)$, moreover, $\text{sg}[\cdot]$ donates the stop gradient (sg) operation, indicating $X_{\text{tgt}}^{\text{m}}(x_t, t, r)$ serves as ground-truth in this loss function and is independent of optimization.

However, the marginal state $x_{t \rightarrow r}$ in Eq.(52) and the marginal velocity $v(x_t, t)$ used in calculation of $\frac{d}{dt} X^\theta(x_t, t, r)$ Eq.(50) are not tractable, so the marginal loss Eq.(51) above cannot be computed as is.

Instead, we minimize conditional Transition Flow Matching loss (C-TFM), which is tractable:

$$\mathcal{L}_{\text{C-TFM}}(\theta) = \mathbb{E}_{t, r, Z, X_t \sim p_t | Z(\cdot | Z)} D\left(\text{sg}[X_{\text{tgt}}^c(X_t, t, r | Z)], X^\theta(X_t, t, r)\right) \quad (53)$$

$$\text{where} \quad X_{\text{tgt}}^c(X_t, t, r | Z) = X_{t \rightarrow r}^Z + (r - t) \frac{d}{dt} X^\theta(X_t, t, r) \quad (54)$$

where the conditional state $x_{t \rightarrow r}^z$ in Eq.(54) and the conditional velocity $v(x_t, t | z)$ used in calculation of $\frac{d}{dt} X^\theta(x_t, t, r)$ Eq.(50) are tractable (see Eq.(57) for details), gives us a computable loss function Eq.(53).

The two losses Eq.(51) and Eq.(53) are equivalent for learning purposes, since their gradients coincide:

Theorem 4 (Gradient equivalence of Transition Flow Matching). *The gradients of the marginal Transition Flow Matching loss and the conditional Transition Flow Matching loss coincide:*

$$\nabla_\theta \mathcal{L}_{\text{M-TFM}}(\theta) = \nabla_\theta \mathcal{L}_{\text{C-TFM}}(\theta) \quad (55)$$

In particular, the minimizer of the conditional Transition Flow Matching loss is the marginal target $X_{\text{tgt}}^m(x_t, t, r)$, which satisfies the Transition Flow Identity Eq.(49).

Proof (Proof of Theorem 4). We show Eq.(55) by a direct computation.

$$\begin{aligned} \nabla_\theta \mathcal{L}_{\text{M-TFM}}(\theta) &= \nabla_\theta \mathbb{E}_{t, r, X_t \sim p_t} D\left(\text{sg}[X_{\text{tgt}}^m(X_t, t, r)], X^\theta(X_t, t, r)\right) \\ &\stackrel{(a)}{=} \mathbb{E}_{t, r, X_t \sim p_t} \nabla_\theta D\left(\text{sg}[X_{\text{tgt}}^m(X_t, t, r)], X^\theta(X_t, t, r)\right) \\ &\stackrel{(b)}{=} \mathbb{E}_{t, r, X_t \sim p_t} \nabla_2 D\left(X_{\text{tgt}}^m(X_t, t, r), X^\theta(X_t, t, r)\right) \nabla_\theta X^\theta(X_t, t, r) \\ &\stackrel{(c)}{=} \mathbb{E}_{t, r, X_t \sim p_t} \nabla_2 D\left(\mathbb{E}_{Z \sim p_Z | t(\cdot | X_t)} [X_{\text{tgt}}^c(X_t, t, r | Z)], X^\theta(X_t, t, r)\right) \nabla_\theta X^\theta(X_t, t, r) \\ &\stackrel{(d)}{=} \mathbb{E}_{t, r, X_t \sim p_t} \mathbb{E}_{Z \sim p_Z | t(\cdot | X_t)} \left[\nabla_2 D\left(X_{\text{tgt}}^c(X_t, t, r | Z), X^\theta(X_t, t, r)\right) \nabla_\theta X^\theta(X_t, t, r) \right] \\ &\stackrel{(e)}{=} \mathbb{E}_{t, r, X_t \sim p_t} \mathbb{E}_{Z \sim p_Z | t(\cdot | X_t)} \left[\nabla_\theta D\left(\text{sg}[X_{\text{tgt}}^c(X_t, t, r | Z)], X^\theta(X_t, t, r)\right) \right] \\ &\stackrel{(f)}{=} \nabla_\theta \mathbb{E}_{t, r, Z, X_t \sim p_t | Z(\cdot | Z)} D\left(\text{sg}[X_{\text{tgt}}^c(X_t, t, r | Z)], X^\theta(X_t, t, r)\right) \\ &= \nabla_\theta \mathcal{L}_{\text{C-TFM}}(\theta). \end{aligned} \quad (56)$$

Explanations of labeled steps.

- (a) Interchange ∇_θ and \mathbb{E} by the Leibniz rule.
- (b) The stop-gradient makes the first argument $\text{sg}[X_{\text{tgt}}^m(X_t, t, r)]$ θ -independent for differentiation, hence the gradient flows only through the second argument. Applying the chain rule yields $\nabla_\theta D(\text{sg}[\cdot], X^\theta) = \nabla_2 D(\cdot, X^\theta) \nabla_\theta X^\theta$.

- (c) Use the definitions Eq.(52) and Eq.(54) together with the marginal–conditional relation for transition states Eq.(44) and velocity Eq.(31):

$$\begin{aligned}
X_{\text{tgt}}^{\text{m}}(X_t, t, r) &= X_{t \rightarrow r} + (r - t) \frac{d}{dt} X^\theta(X_t, t, r) \\
&= X(X_t, t, r) + (r - t) \frac{d}{dt} X^\theta(X_t, t, r) \\
&= X(X_t, t, r) + (r - t) \left(\partial_{X_t} X^\theta(X_t, t, r) \cdot v(X_t, t) + \partial_t X^\theta(X_t, t, r) \right) \\
&= \mathbb{E}_{Z \sim p_{Z|t}(\cdot|X_t)} \left[X(X_t, t, r | Z) + (r - t) \left(\partial_{X_t} X^\theta(X_t, t, r) \cdot v(X_t, t | Z) \right. \right. \\
&\quad \left. \left. + \partial_t X^\theta(X_t, t, r) \right) \right] \\
&= \mathbb{E}_{Z \sim p_{Z|t}(\cdot|X_t)} \left[X(X_t, t, r | Z) + (r - t) \frac{d}{dt} X^\theta(X_t, t, r) \right] \\
&= \mathbb{E}_{Z \sim p_{Z|t}(\cdot|X_t)} \left[X_{t \rightarrow r}^Z + (r - t) \frac{d}{dt} X^\theta(X_t, t, r) \right] \\
&= \mathbb{E}_{Z \sim p_{Z|t}(\cdot|X_t)} \left[X_{\text{tgt}}^{\text{c}}(X_t, t, r | Z) \right],
\end{aligned} \tag{57}$$

where $\partial_{X_t} X^\theta(X_t, t, r)$ and $\partial_t X^\theta(X_t, t, r)$ are Z -independent given (X_t, t, r) .

- (d) Since $D(\cdot, \cdot)$ is a Bregman divergence, its gradient with respect to the second argument, $\nabla_2 D(a, b)$, is affine in the first argument a for fixed b . Conditioning on X_t , this implies the (conditional) expectation can be moved inside:

$$\nabla_2 D\left(\mathbb{E}[A | X_t], b\right) = \mathbb{E}[\nabla_2 D(A, b) | X_t].$$

Apply this with $A = X_{\text{tgt}}^{\text{c}}(X_t, t, r | Z)$ and $b = X^\theta(X_t, t, r)$.

- (e) Reverse the chain rule as in (b): because $\text{sg}[X_{\text{tgt}}^{\text{c}}]$ freezes the first argument, we have $\nabla_2 D(\cdot, X^\theta) \nabla_\theta X^\theta = \nabla_\theta D(\text{sg}[\cdot], X^\theta)$.
- (f) Use Bayes' rule to swap the sampling orders:

$$\mathbb{E}_{X_t \sim p_t} \mathbb{E}_{Z \sim p_{Z|t}(\cdot|X_t)}[\cdot] = \mathbb{E}_Z \mathbb{E}_{X_t \sim p_{t|Z}(\cdot|Z)}[\cdot],$$

and interchange ∇_θ with \mathbb{E} (as in (a)) to recognize $\nabla_\theta \mathcal{L}_{\text{C-TFM}}(\theta)$ in Eq.(53).

Therefore, $\nabla_\theta \mathcal{L}_{\text{M-TFM}}(\theta) = \nabla_\theta \mathcal{L}_{\text{C-TFM}}(\theta)$, which proves Eq.(55). \square

Remark 4 (Minimizer). Since the two objectives Eq.(51) and Eq.(53) have identical gradients, they share the same stationary points. Moreover, because

$$X_{\text{tgt}}^{\text{m}}(X_t, t, r) = \mathbb{E}_{Z \sim p_{Z|t}(\cdot|X_t)} \left[X_{\text{tgt}}^{\text{c}}(X_t, t, r | Z) \right],$$

the conditional objective Eq.(53) regresses $X^\theta(X_t, t, r)$ toward the marginal target $X_{\text{tgt}}^{\text{m}}(X_t, t, r)$, and $X_{\text{tgt}}^{\text{m}}$ is defined to satisfy the **Transition Flow Identity** Eq.(49).

8.5 Training Transition Flow Matching Model

Building on the previous development, we now have all the ingredients required to train a Transition Flow Matching model. We inherit the setting in Remark 3 by taking $Z = (X_0, X_1)$ and using the linear interpolant $X_t = (1 - t)X_0 + tX_1$, which yields a concrete, standard form of Transition Flow Matching.

Remark 5 (Standard Transition Flow Matching). We adopt the standard Flow Matching setting in Remark 3 by setting $Z = (X_0, X_1)$, and use the linear interpolant

$$X_t = (1 - t)X_0 + tX_1, \quad 0 \leq t \leq 1.$$

For any $0 \leq t \leq r \leq 1$, the conditional transition state is

$$X_{t \rightarrow r}^Z = (1 - r)X_0 + rX_1,$$

and the conditional velocity is constant:

$$v(X_t, t | Z) = X_1 - X_0.$$

The tractable Transition Flow Matching objective in Eq.(53) can be written explicitly as

$$\mathcal{L}_{\text{TFM}}(\theta) = \mathbb{E}_{t, r, Z, X_t \sim p_{t|Z}(\cdot|Z)} D\left(\text{sg}[X_{t \rightarrow r}^Z + (r - t)\frac{d}{dt}X^\theta(X_t, t, r)], X^\theta(X_t, t, r)\right) \quad (58)$$

$$\text{where } \frac{d}{dt}X^\theta(X_t, t, r) = \partial_{x_t}X^\theta(X_t, t, r) \cdot v(X_t, t | Z) + \partial_t X^\theta(X_t, t, r) \quad (59)$$

During inference, we recursively apply the model to transform the generation trajectory from the source distribution to the target distribution:

$$\hat{x}_r = X^\theta(x_t, t, r) \quad (60)$$

For clarity, we summarize the conceptual training and inference procedures in Algorithm 2 and Algorithm 3. In particular, by extending Algorithm 3, the one-step generation procedure is described in Algorithm 4.

References

1. Albergo, M.S., Boffi, N.M., Vanden-Eijnden, E.: Stochastic interpolants: A unifying framework for flows and diffusions, 2023. URL <https://arxiv.org/abs/2303.08797> **3** (2023)
2. Albergo, M.S., Vanden-Eijnden, E.: Building normalizing flows with stochastic interpolants. In: The Eleventh International Conference on Learning Representations (2023), <https://openreview.net/forum?id=li7qeBbCR1t>
3. Boffi, N.M., Albergo, M.S., Vanden-Eijnden, E.: Flow map matching. arXiv preprint arXiv:2406.07507 **2**(3), 9 (2024)
4. Cai, S., Chan, E.R., Zhang, Y., Guibas, L., Wu, J., Wetzstein, G.: Diffusion self-distillation for zero-shot customized image generation. In: Proceedings of the Computer Vision and Pattern Recognition Conference. pp. 18434–18443 (2025)
5. Dormand, J.R., Prince, P.J.: A family of embedded runge-kutta formulae. Journal of computational and applied mathematics **6**(1), 19–26 (1980)

Algorithm 2 Transition Flow Matching (TFM): Training

```

Note: In PyTorch and JAX, jvp returns (function_output, JVP).
// tfm(x_t, t, r): uses model  $X^\theta(x_t, t, r)$  predicting the transition
state at time r
// metric(.): e.g., MSE, any Bregman divergence on residuals

x_1 = sample_from_training_batch()           // sample from target
distribution  $p_1$ 
x_0 = randn_like(x_1)                       // sample from source distribution  $p_0$ 
(Gaussian), independent of  $p_1$ 
(t, r) = sample_t_r()                       //  $0 \leq t \leq r \leq 1$ 

x_t = (1 - t)x_0 + tx_1                     // current state
v = x_1 - x_0                               // conditional velocity with  $Z = (X_0, X_1)$ 
x_t_to_r = (1 - r)x_0 + rx_1 // conditional transition state with  $Z$ 
=  $(X_0, X_1)$ 

(X, dX_dt) = jvp(tfm, (x_t, t, r), (v, 1, 0)) //  $d/dt X^\theta =$ 
partial_x  $X^\theta * v +$  partial_t  $X^\theta$ 

X_tgt = x_t_to_r + (r - t)dX_dt
error = X - stopgrad(X_tgt)
loss = metric(error)

return loss

```

6. Dosovitskiy, A., Beyer, L., Kolesnikov, A., Weissenborn, D., Zhai, X., Unterthiner, T., Dehghani, M., Minderer, M., Heigold, G., Gelly, S., Uszkoreit, J., Houlsby, N.: An image is worth 16x16 words: Transformers for image recognition at scale (2021), <https://arxiv.org/abs/2010.11929>
7. Esser, P., Kulal, S., Blattmann, A., Entezari, R., Müller, J., Saini, H., Levi, Y., Lorenz, D., Sauer, A., Boesel, F., Podell, D., Dockhorn, T., English, Z., Rombach, R.: Scaling rectified flow transformers for high-resolution image synthesis. In: Forty-first International Conference on Machine Learning (2024), <https://openreview.net/forum?id=FPnUhsQJ5B>
8. Esser, P., Kulal, S., Blattmann, A., Entezari, R., Müller, J., Saini, H., Levi, Y., Lorenz, D., Sauer, A., Boesel, F., Podell, D., Dockhorn, T., English, Z., Lacey, K., Goodwin, A., Marek, Y., Rombach, R.: Scaling rectified flow transformers for high-resolution image synthesis (2024), <https://arxiv.org/abs/2403.03206>
9. Frans, K., Hafner, D., Levine, S., Abbeel, P.: One step diffusion via shortcut models. In: The Thirteenth International Conference on Learning Representations (2025), <https://openreview.net/forum?id=0lzB6LnXcS>
10. Geng, Z., Deng, M., Bai, X., Kolter, J.Z., He, K.: Mean flows for one-step generative modeling. arXiv preprint arXiv:2505.13447 (2025)

Algorithm 3 TFM: Multi-step Sampling with Arbitrary Step Sizes

```

// Choose any time grid:  $0 = t_0 < t_1 < \dots < t_K = 1$ 

x = randn(x_shape) // x = x_{t_0} = x_0

for k = 0 to K - 1:
    t = t_k, r = t_{k+1}
    x = tfm(x, t, r) // x = x_{t_to_r}

return x // x = x_{t_K} = x_1

```

Algorithm 4 TFM: 1-step Sampling

```

x = randn(x_shape)
// x = x_0
x = tfm(x, 0, 1) //
x = x_1

return x

```

11. Geng, Z., Lu, Y., Wu, Z., Shechtman, E., Kolter, J.Z., He, K.: Improved mean flows: On the challenges of fastforward generative models. arXiv preprint arXiv:2512.02012 (2025)
12. Geng, Z., Pokle, A., Kolter, J.Z.: One-step diffusion distillation via deep equilibrium models. In: Thirty-seventh Conference on Neural Information Processing Systems (2023), <https://openreview.net/forum?id=b6XvK2de99>
13. Geng, Z., Pokle, A., Luo, W., Lin, J., Kolter, J.Z.: Consistency models made easy. In: The Thirteenth International Conference on Learning Representations (2025), <https://openreview.net/forum?id=xQVxo9dSID>
14. Guo, P., Schwing, A.: Variational rectified flow matching. In: Forty-second International Conference on Machine Learning (2025), <https://openreview.net/forum?id=Rk18ZikrFI>
15. Heusel, M., Ramsauer, H., Unterthiner, T., Nessler, B., Hochreiter, S.: Gans trained by a two time-scale update rule converge to a local nash equilibrium. Advances in neural information processing systems **30** (2017)
16. Ho, J., Salimans, T.: Classifier-free diffusion guidance (2022), <https://arxiv.org/abs/2207.12598>
17. Hu, Z., Lai, C.H., Mitsufuji, Y., Ermon, S.: Cmt: Mid-training for efficient learning of consistency, mean flow, and flow map models. arXiv preprint arXiv:2509.24526

- (2025)
18. Karras, T., Aittala, M., Aila, T., Laine, S.: Elucidating the design space of diffusion-based generative models. *Advances in neural information processing systems* **35**, 26565–26577 (2022)
 19. Kim, D., Lai, C.H., Liao, W.H., Murata, N., Takida, Y., Uesaka, T., He, Y., Mitsufuji, Y., Ermon, S.: Consistency trajectory models: Learning probability flow ODE trajectory of diffusion. In: *The Twelfth International Conference on Learning Representations* (2024), <https://openreview.net/forum?id=ymjI8feDTD>
 20. Kim, D., Lai, C.H., Liao, W.H., Murata, N., Takida, Y., Uesaka, T., He, Y., Mitsufuji, Y., Ermon, S.: Consistency trajectory models: Learning probability flow ode trajectory of diffusion (2024), <https://arxiv.org/abs/2310.02279>
 21. Klein, L., Krämer, A., Noé, F.: Equivariant flow matching. *Advances in Neural Information Processing Systems* **36**, 59886–59910 (2023)
 22. Krizhevsky, A., Hinton, G., et al.: Learning multiple layers of features from tiny images (2009)
 23. Krizhevsky, A., Sutskever, I., Hinton, G.E.: Imagenet classification with deep convolutional neural networks. *Advances in neural information processing systems* **25** (2012)
 24. Lai, C.H., Song, Y., Kim, D., Mitsufuji, Y., Ermon, S.: The principles of diffusion models (2025), <https://arxiv.org/abs/2510.21890>
 25. Lee, S., Lin, Z., Fanti, G.: Improving the training of rectified flows. *Advances in neural information processing systems* **37**, 63082–63109 (2024)
 26. Lipman, Y., Chen, R.T.Q., Ben-Hamu, H., Nickel, M., Le, M.: Flow matching for generative modeling. In: *The Eleventh International Conference on Learning Representations* (2023), <https://openreview.net/forum?id=PqvMRDCJT9t>
 27. Lipman, Y., Havasi, M., Holderrieth, P., Shaul, N., Le, M., Karrer, B., Chen, R.T.Q., Lopez-Paz, D., Ben-Hamu, H., Gat, I.: Flow matching guide and code (2024), <https://arxiv.org/abs/2412.06264>
 28. Lipman, Y., Havasi, M., Holderrieth, P., Shaul, N., Le, M., Karrer, B., Chen, R.T., Lopez-Paz, D., Ben-Hamu, H., Gat, I.: Flow matching guide and code. *arXiv preprint arXiv:2412.06264* (2024)
 29. Liu, X., Gong, C., qiang liu: Flow straight and fast: Learning to generate and transfer data with rectified flow. In: *The Eleventh International Conference on Learning Representations* (2023), <https://openreview.net/forum?id=XVjTT1nw5z>
 30. Lu, C., Song, Y.: Simplifying, stabilizing and scaling continuous-time consistency models. In: *The Thirteenth International Conference on Learning Representations* (2025), <https://openreview.net/forum?id=LyJi5ugyJx>
 31. Lu, Y., Lu, S., Sun, Q., Zhao, H., Jiang, Z., Wang, X., Li, T., Geng, Z., He, K.: One-step latent-free image generation with pixel mean flows. *arXiv preprint arXiv:2601.22158* (2026)
 32. Luo, T., Yuan, H., Liu, Z.: Soflow: Solution flow models for one-step generative modeling. *arXiv preprint arXiv:2512.15657* (2025)
 33. Ma, C., Xiao, X., Wang, T., Shen, Y.: Beyond editing pairs: Fine-grained instructional image editing via multi-scale learnable regions. *arXiv preprint arXiv:2505.19352* (2025)
 34. Ma, C., Xiao, X., Wang, T., Wang, X., Shen, Y.: CAD-VAE: Leveraging correlation-aware latents for comprehensive fair disentanglement. In: *The Fortieth AAAI Conference on Artificial Intelligence* (2025)
 35. Ma, C., Xiao, X., Wang, T., Wang, X., Shen, Y.: Stochastic interpolants via conditional dependent coupling. *arXiv preprint arXiv:2509.23122* (2025)

36. Ma, C., Xiao, X., Wang, T., Wang, X., Shen, Y.: Learning straight flows: Variational flow matching for efficient generation (2026), <https://arxiv.org/abs/2511.17583>
37. Ma, N., Goldstein, M., Albergo, M.S., Boffi, N.M., Vanden-Eijnden, E., Xie, S.: Sit: Exploring flow and diffusion-based generative models with scalable interpolant transformers. In: European Conference on Computer Vision. pp. 23–40. Springer (2024)
38. Nie, W., Berner, J., Ma, N., Liu, C., Xie, S., Vahdat, A.: Transition matching distillation for fast video generation. arXiv preprint arXiv:2601.09881 (2026)
39. Rombach, R., Blattmann, A., Lorenz, D., Esser, P., Ommer, B.: High-resolution image synthesis with latent diffusion models (2022), <https://arxiv.org/abs/2112.10752>
40. Sabour, A., Fidler, S., Kreis, K.: Align your flow: Scaling continuous-time flow map distillation. arXiv preprint arXiv:2506.14603 (2025)
41. Salimans, T., Ho, J.: Progressive distillation for fast sampling of diffusion models. In: International Conference on Learning Representations (2022), <https://openreview.net/forum?id=TIIXIpzhoI>
42. Silvestri, G., Ambrogioni, L., Lai, C.H., Takida, Y., Mitsufuji, Y.: VCT: Training consistency models with variational noise coupling. In: Forty-second International Conference on Machine Learning (2025), <https://openreview.net/forum?id=CMoXOBESDs>
43. Song, Y., Dhariwal, P.: Improved techniques for training consistency models. In: The Twelfth International Conference on Learning Representations (2024), <https://openreview.net/forum?id=WNzy9bRDvG>
44. Song, Y., Dhariwal, P., Chen, M., Sutskever, I.: Consistency models. In: Proceedings of the 40th International Conference on Machine Learning. pp. 32211–32252 (2023)
45. Song, Y., Sohl-Dickstein, J., Kingma, D.P., Kumar, A., Ermon, S., Poole, B.: Score-based generative modeling through stochastic differential equations. In: International Conference on Learning Representations (2021), <https://openreview.net/forum?id=PXTIG12RRHS>
46. Tong, A., Fatras, K., Malkin, N., Huguet, G., Zhang, Y., Rector-Brooks, J., Wolf, G., Bengio, Y.: Improving and generalizing flow-based generative models with mini-batch optimal transport. arXiv preprint arXiv:2302.00482 (2023)
47. Vaswani, A., Shazeer, N., Parmar, N., Uszkoreit, J., Jones, L., Gomez, A.N., Kaiser, L., Polosukhin, I.: Attention is all you need (2023), <https://arxiv.org/abs/1706.03762>
48. Wang, F.Y., Yang, L., Huang, Z., Wang, M., Li, H.: Rectified diffusion: Straightness is not your need in rectified flow. arXiv preprint arXiv:2410.07303 (2024)
49. Wang, Z., Zhang, Y., Yue, X., Yue, X., Li, Y., Ouyang, W., Bai, L.: Transition models: Rethinking the generative learning objective. arXiv preprint arXiv:2509.04394 (2025)
50. Zhang, H., Siarohin, A., Menapace, W., Vasilkovsky, M., Tulyakov, S., Qu, Q., Skorokhodov, I.: Alphaflow: Understanding and improving meanflow models. arXiv preprint arXiv:2510.20771 (2025)
51. Zhang, Y., Yan, Y., Schwing, A., Zhao, Z.: Hierarchical rectified flow matching with mini-batch couplings. arXiv preprint arXiv:2507.13350 (2025)
52. Zhang, Y., Yan, Y., Schwing, A., Zhao, Z.: Towards hierarchical rectified flow. In: The Thirteenth International Conference on Learning Representations (2025), <https://openreview.net/forum?id=6F6qwdycgJ>

53. Zhou, L., Ermon, S., Song, J.: Inductive moment matching. In: Forty-second International Conference on Machine Learning (2025), <https://openreview.net/forum?id=pwNSUo7yUb>